Pattern-Informed Energetics: Inferring energy allocation and the emergence of life-history strategies

Authors: Cara A. Gallagher[1,2*], Viktoriia Radchuk[3], Melanie Dammhahn[4,5], & Florian Jeltsch[1]

[1]Plant Ecology and Nature Conservation, Institute of Biochemistry and Biology, University of Potsdam, 14469 Potsdam, Germany.

[2]Department of Ecoscience, Aarhus University, 4000 Roskilde, Denmark.

[3]Leibniz Institute for Zoo and Wildlife Research, Alfred-Kowalke-Straße 17, Berlin, Germany.

[4]Behavioural Biology, Institute for Neuro- and Behavioural Biology, University of Münster, Badestrasse 9, 48149 Münster, Germany

[5]Joint Institute for Individualisation in a Changing Environment (JICE), University of Münster and Bielefeld University, Germany

*__Corresponding author:__ Cara Gallagher; Frederiksborgvej 399, 4000 Roskilde, Denmark; cara.gallagher@ecos.au.dk; +45 50190332

Acknowledgements: We extend our gratitude to Victoria Boult for valuable early discussions that contributed to the development of scenarios. Additionally, we thank Herman Pontzer for his insightful discussions on modeling animal energy budgets and allocation, which greatly inspired this work. Funding for this study was provided by the DFG-funded research training group 'BioMove' (Deutsche Forschungsgemeinschaft Grant GRK 2118) (CAG, VR, MD, FJ).

Conflict of interest: The authors have no conflicts of interest to report.

Author contributions:

Conceptualization: CAG, VR, MD, FJ

Data curation: CAG

Methodology: CAG, VR, MD, FJ

Formal analysis: CAG

Visualization: CAG
Funding acquisition: FJ
Supervision: FJ
Writing—original draft: CAG
Writing—review & editing: CAG, VR, MD, FJ

Statement on inclusion: Our study used a modeling approach based on secondary data, rather than primary data, meaning no local data collection was conducted. Most of the case study data were derived from extensive research on bank voles across Europe, with example scenarios serving as illustrations. However, for detailed site-specific projections, local involvement would undoubtedly enhance these predictions, particularly in areas such as local forage availability.

Data accessibility statement: All data, code, and materials used in the analyses are made available for download on Figshare at:
https://figshare.com/s/f68336510e6fb8201613

Abstract

Energy allocation among survival, growth, and reproduction is central to population dynamics, yet remains difficult to quantify directly. Traditional models often rely on fixed rules or optimization assumptions that may not capture real-world variability. We introduce Pattern-Informed Energetics (PIE), a framework that infers allocation strategies from empirical data using inverse parameterization. We applied PIE at two scales: a cross-species study of six mammals spanning a 1,000-fold mass range and a spatially explicit population model of the bank vole (*Myodes glareolus*). Cross-species results revealed strong allometric scaling in allocation midpoints, with larger mammals shifting energy to growth and reproduction at higher body conditions. In the bank vole model, PIE reproduced complex field and experimental patterns, including seasonal dynamics and the effects of litter manipulation on reproductive costs and maternal survival. While life-history patterns effectively constrained

allocation midpoints, the steepness of the energetic response was more difficult to infer, highlighting specific data needs for future studies. PIE provides a flexible, transparent approach to bioenergetic modeling, quantifying uncertainty and revealing how evolved life-history strategies emerge from energetic constraints, thereby improving predictions of species' responses to environmental change.

Introduction

Energy allocation among survival, growth, and reproduction is fundamental to animal fitness and population dynamics (Glazier, 2008), yet remains a challenging process to measure directly. Although some energetic fluxes, such as changes in body mass, milk production, food intake, metabolic rates, or shifts in organ masses under environmental change, can be measured or estimated (Gittleman & Thompson, 1988; Glazier, 2008), these observations represent proximate outcomes of allocation rather than the underlying decision rules that govern how energy is partitioned among competing functions (Pontzer & McGrosky, 2022). Even in well-studied taxa, the internal process through which animals allocate limited energy, and how this process shifts with nutritional state or physiological demands, remains largely unknown (McHuron et al., 2022; Sibly et al., 2013).

In life-history theory, animal metabolic processes are viewed as evolutionary adaptations shaped by environmental conditions, with limited resources allocated among competing demands under trait trade-offs (Ricklefs & Wikelski, 2002; White et al., 2022). Environmental change can disrupt both energy acquisition and allocation, compromising fitness (e.g., Clairbaux et al., 2021). Understanding these trade-offs is therefore essential for predicting population responses to environmental stressors (Sibly et al., 2013).

Energy budget models have been applied for over 70 years to address diverse questions, from fisheries management to climate impacts on wildlife (Boult et al., 2019; Boyd et al., 2018; Winberg, 1956). However, approaches vary substantially in their assumptions about allocation. Dynamic Energy Budget (DEB) theory assumes fixed

allocation fractions (Kooijman, 2000), hierarchical models prioritize maintenance over growth and reproduction (Sibly et al., 2013), while optimization approaches assume animals allocate energy in a manner that maximizes fitness (McNamara & Houston, 1996). While each framework offers important strengths, most do not explicitly resolve the context-dependence of allocation rules, nor do they accommodate consideration of uncertainty in these processes.

A key gap remains: how do we parameterize allocation strategies under variable conditions without arbitrary thresholds or untested optimality assumptions? Observing allocation processes *per se* remains infeasible in wildlife, and even directly related empirical patterns, such as reproductive performance across body condition gradients, are still scarce (but see (Beltran et al., 2023; Bright Ross et al., 2021; Christiansen et al., 2014; Lamb et al., 2023; Van Benthem et al., 2017). However, emerging technological and analytical tools provide new opportunities. Pattern-oriented modeling (POM) and statistical inference methods (Gallagher, Chudzinska, et al., 2021; Grimm & Railsback, 2012; Hartig et al., 2011) make it possible to estimate otherwise unobtainable parameters by matching models to multiple empirical patterns. In this way, allocation strategies need not be assumed in advance but can instead be inferred from the empirical outcomes they produce.

The key insight is that while allocation processes are unmeasurable, their *consequences* are widely observed. We can measure morphometrics (e.g., body mass, composition), life history traits (e.g., age at maturity, reproductive output, longevity), energetics (e.g., metabolic rates, food intake), and population dynamics (e.g., density, survival rates). Each pattern contains integrated information about the allocation processes that produced it (e.g. task -> trait relationships in Pontzer & McGrosky, 2022). By calibrating mechanistic energy budget models to reproduce multiple of such patterns simultaneously, we can infer the allocation strategies that underlie observed outcomes.

Here, we introduce the Pattern-Informed Energetics (PIE) framework, which derives energy allocation strategies directly from empirical patterns through inverse parameterization. Rather than prescribing fixed allocation rules, PIE allows allocation

to emerge as condition-dependent relationships, shaped by body reserves, reproductive state, and resource availability, that are constrained by empirical observations. This approach explicitly incorporates uncertainty, as resulting parameter distributions reflect the range of allocation strategies consistent with observed patterns, revealing both what we can confidently infer and what requires additional information.

PIE offers several advantages over traditional approaches: (1) it avoids arbitrary allocation rules while remaining mechanistic, (2) it grounds allocation dynamics in empirical reality, (3) it quantifies uncertainty in allocation processes explicitly, (4) it reveals which allocation parameters can and cannot be constrained by available data, and (5) it is applicable to any underlying energy budget framework where allocation strategies can be expressed as functions of physiological state.

We demonstrate PIE's utility through two complementary applications that address distinct but necessary questions: whether energetic allocation strategies can be inferred from aggregate life-history patterns, and whether such inferred strategies generate predictive power in complex, heterogeneous systems. We demonstrate PIE's utility through two complementary applications. First, we apply a simple cross-species energy-budget model to six mammal species spanning a 1,000-fold body-mass variation (18 g mouse to >6 kg raccoon). Using just five commonly available life-history patterns per species (adult mass, birth mass, weaning mass, age at maturity, lifespan), we derive allocation strategies and examine whether emergent parameter relationships align with life-history theory. This demonstration reveals PIE's capacity to recover theoretical predictions from empirical constraints and identifies which allocation parameters can and cannot be constrained by aggregate patterns.

Second, we develop a detailed spatially explicit individual-based model for bank voles (*Myodes glareolus*), calibrating allocation parameters to 16 empirical patterns spanning morphometrics, energetics, life history, reproduction, and population dynamics. We validate the model's predictive capacity by testing it against 24 additional patterns, including independent replication of a real-world litter

manipulation experiment (Koivula et al., 2003), testing whether allocation strategies derived from observational patterns can predict outcomes of experimental interventions across environmental contexts. This application demonstrates PIE's scalability to complex systems and its ability to generate testable predictions.

Together, these demonstrations illustrate when and how PIE can inform bioenergetic models. We provide practical guidance on pattern selection, calibration approaches, and interpretation of parameter uncertainties. We discuss data requirements for constraining different allocation processes, compare PIE conceptually to alternative frameworks, and identify opportunities for future development.

By leveraging diverse empirical knowledge to infer parameters governing some of the most elusive yet vital processes driving animal fitness (McHuron et al., 2022; Sibly et al., 2013), PIE offers a transparent, data-driven approach to parameterizing energy allocation that can improve predictions of species responses to environmental change.

Methods

Pattern-Informed Energetics (PIE) infers energy allocation strategies by fitting a mechanistic energy-budget model to the observable consequences of allocation, rather than prescribing how organisms ought to allocate energy. In practice, PIE consists of three main steps: (1) specifying a mechanistic bioenergetic model linking metabolism, growth, reproduction, and survival; (2) representing allocation behavior using flexible, parameterized functions; and (3) inferring allocation parameters via inverse parameterization to reproduce multiple empirical patterns simultaneously.

The underlying bioenergetic model tracks energy acquisition and expenditure across maintenance, growth, and reproduction, with survival governed by condition-dependent physiological limits. Allocation behavior is represented using sigmoidal functions that map body condition to allocation priorities (Figure 1). The parameters of these functions correspond to biologically interpretable decision

points, including where allocation shifts away from growth, when reproduction becomes viable, and how sharply mortality risk increases as condition declines.

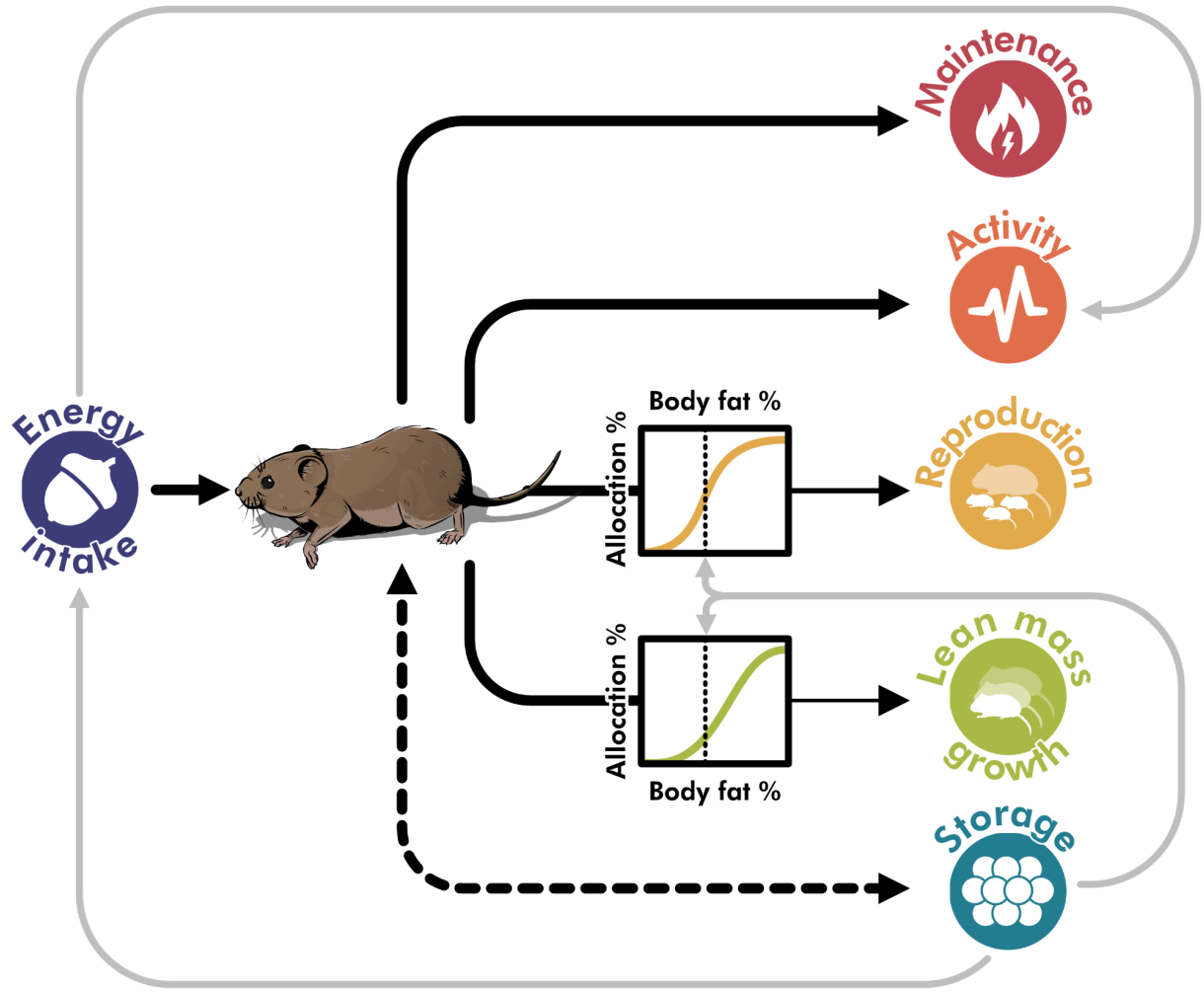

Figure 1. Schematic showing key processes in the energy-allocation framework, with light grey lines indicating interactions. Sigmoidal growth and reproduction curves depict energy allocation to each process. In the PIE approach, allocation follows body-condition-dependent relationships calibrated to empirical patterns.

Allocation parameters are estimated using inverse parameterization, whereby model outputs are matched to multiple empirical patterns, including morphometrics, energetics, life-history traits, and population-level dynamics. Inference is performed using uncertainty-aware methods such as Approximate Bayesian Computation

(ABC), likelihood-based Bayesian approaches, or Generalized Likelihood Uncertainty Estimation (GLUE; Beven & Binley, 2014; van der Vaart et al., 2016, 2018). These approaches yield posterior distributions over allocation parameters, rather than single best-fit values, thereby explicitly quantifying uncertainty in inferred strategies.

Although allocation decisions themselves are unobserved, their downstream effects are measurable. Growth trajectories inform allocation to somatic growth, reproductive output reflects reproductive investment, and survival outcomes constrain physiological limits. By requiring the model to reproduce multiple patterns simultaneously, PIE restricts parameter space to energetically feasible allocation strategies supported by the data. Different classes of empirical patterns constrain different components of allocation, with growth data primarily informing growth investment, reproductive metrics defining reproductive thresholds, and population-level patterns integrating survival and energetic trade-offs over time.

Crucially, PIE makes uncertainty transparent. Posterior distributions reveal which allocation parameters are tightly constrained by existing data and which remain weakly identifiable. This, in turn, highlights the types of measurements most likely to improve inference, such as body-condition–dependent growth rates, reproductive performance under variable nutritional states, or detailed survival curves.

Representing Energy Allocation

Body fat and other energy reserves integrate recent intake and expenditure, serving as a physiological buffer for costly life-history processes. Because reproduction, growth, and survival draw on limited energy stores, individuals with higher reserves show higher pregnancy probabilities, faster juvenile growth, and greater survival, whereas depleted reserves are linked to reduced reproductive success and lower juvenile survival. For example, in ungulates, body fat strongly predicts pregnancy probability, offspring growth, twinning rates, and juvenile survival (Lamb et al., 2023; Parker et al., 2009; Stephenson et al., 2020; Tollefson et al., 2010), illustrating that stored energy underpins key fitness components in wild mammal populations.

In both demonstrations presented here, we model allocation as sigmoid functions of body fat percentage:

$$Allocation[Prop] = \frac{1}{1 + \exp\left(-k_i \left(\frac{SL}{SL_{\max}} - x_{i,0}\right)\right)}$$

where k_i is steepness (sensitivity of allocation to condition), $x_{i,0}$ is the midpoint (threshold body condition for 50% allocation), SL is current body fat percentage, and SL_{max} is maximum sustainable body fat. Each allocation process (growth, pregnancy, lactation, survival) has unique steepness and midpoint parameters.

Sigmoid functions are deemed biologically realistic, as recent empirical studies demonstrate non-linear reproductive responses to body condition in diverse mammals (Archer et al., 2023; Beltran et al., 2023; Bright Ross et al., 2021). When body fat is below the midpoint, allocation to that process is reduced; when above, allocation approaches maximum capacity (defined from observed or extreme physiological values; see Demonstrations). Steep curves create sharp threshold responses, while shallow curves produce gradual allocation changes across a wider body condition range.

Allocation modulates processes differently depending on model structure. For growth, allocation can scale both instantaneous growth rate and effective asymptotic mass, so animals in poor condition grow more slowly *and* mature at smaller sizes. For reproduction, allocation scales the proportion of calculated costs that mothers invest, representing reduced litter sizes, lower offspring quality, or reproductive skipping. For survival, the sigmoid represents mortality risk as a function of energy status.

Critically, specific allocation strategies are not assumed but rather *inferred* from empirical patterns through calibration. This allows allocation to vary flexibly with condition in ways that reflect species' evolved life histories and environmental contexts, while remaining grounded in mechanistic energetic constraints. The following demonstrations illustrate how PIE reveals allocation strategies across

species (Demonstration 1) and tests predictions against experimental interventions (Demonstration 2).

Demonstration 1: Cross-Species Allocation Patterns

We implemented a mechanistic daily time-step energy-budget model for a single female mammal from weaning through adulthood to illustrate the PIE framework and fit to commonly available datasets. The model tracks structural mass, fat stores, reproductive state, offspring mass, and survival, with all state variables, parameters, and equations documented in Appendix Tables S1–S3.

Maintenance metabolism scales allometrically with lean body mass using species-specific normalization constants derived from basal metabolic rate data (PanTHERIA; Jones et al., 2009). Daily energy intake is computed based on total energetic demands and a species-specific target body-fat percentage (set as a normal distribution centered on observed values for the species with a standard deviation of 5%), adjusted by a net assimilation efficiency (80%) and a foraging overhead (10%). Growth dynamics follow a Gompertz function, with the rate parameter scaling allometrically with adult mass (Zullinger et al., 1984). Structural growth and tissue-synthesis energetics follow standard bioenergetic assumptions, with values defined in the parameter table (Appendix Table S2). Reproductive costs include maternal support of embryonic growth and fetal maintenance during pregnancy, as well as offspring growth and maintenance during lactation. Embryonic growth parameters are drawn from Ricklefs (2010). Reproductive timing follows species-specific gestation length, lactation duration, and interbirth interval. For generality, all growth-related processes were scaled to allow individuals to exceed typical database values (e.g., up to double adult, neonate, and offspring masses), while calibration ensured that realized trajectories matched observed species traits. This flexible scaling produces biologically plausible curves and can be further refined when species-specific data on exceptional growth are available, as demonstrated in Demonstration 2.

To estimate body mass at sexual maturity, we first used the reported age at sexual maturity. A species-specific Gompertz curve for body growth was then fitted using

birth mass, weaning mass, and the estimated 95% of adult mass at physical maturity. The fitted growth curve was evaluated at the age of sexual maturity to obtain the corresponding maturity mass, which triggers the onset of reproduction in the model. This ensures that individuals must reach sufficient size to reproduce at the observed age.

Individuals die if a daily random draw exceeds their survival probability or if fat reserves reach zero.

Species and Data

We selected six mammal species from the PanTHERIA database (Jones et al., 2009) spanning a 1,000-fold body-mass range: *Peromyscus leucopus*, *Microtus oeconomus*, *Callithrix jacchus*, *Ondatra zibethicus*, *Didelphis marsupialis*, and *Procyon lotor*. Five empirical calibration patterns were used: adult mass (g), neonate mass (g), weaning mass (g), age at sexual maturity (days), and maximum longevity (days). Additional species traits, basal metabolic rate, gestation length, lactation duration, interbirth interval, and litter size, parameterized the energy-budget model (Appendix Table S2). Species-specific body-fat percentages came from Pitts & Bullard (1968). The six selected species represent the subset for which all required life-history, energetic, and body-fat parameters were jointly available across the PanTHERIA database and Pitts & Bullard (1968).

Model Calibration

For each species, we inferred allocation-curve parameters using ABC with rejection sampling (van der Vaart et al., 2016). One million parameter sets were generated using Latin hypercube sampling (McKay, 1992). Prior bounds for steepness and midpoint parameters are listed in Appendix Table S2. The survival-curve midpoint was restricted to the species-specific target fat percentage to avoid unrealistic starvation thresholds and reduce the prevalence of failed simulations.

Each parameter set was evaluated using three replicate simulations from weaning to maximum longevity. We measured model–data agreement across the five calibration

patterns using the root sum of squared relative errors across the calibration patterns ($D=\sqrt{\sum_{i=1}^{n}(\frac{sim_i-obs_i}{obs_i})^2}$; where *D* is the total distance for the parameter set and *n* is the total number of patterns, here 5). For each species, the ten parameter sets with the lowest distance scores were retained as the posterior sample. Retaining multiple sets allowed us to capture parameter uncertainty while preserving the best-fitting solutions.

Analysis

Posterior parameter distributions were used to identify allocation functions constrained by the calibration patterns. Allometric relationships between inferred parameters and adult mass were assessed with Spearman correlations across species and retained parameter sets. Emergent allocation strategies were summarized by plotting allocation functions for growth, pregnancy, lactation, and survival across body-condition gradients for well-fitting parameter sets. Model outputs corresponding to these retained sets were evaluated against the calibration patterns, with uncertainty summarized as 50% and 90% posterior intervals.

All analyses were performed in R v4.4.2 (R Core Team, 2024), with code and data fully available (see Data Accessibility Statement).

Demonstration 2: Single-Species Validation with Experimental Data

To evaluate PIE in a data-rich and ecologically realistic setting, we extended the framework to bank voles. Bank voles offer three advantages: rich empirical datasets, including numerous published patterns spanning morphology, energetics, life history, reproduction, and population dynamics; independent experimental data for validation, notably from litter-manipulation studies (e.g., Koivula et al., 2003); and ecological relevance, given their well-studied population cycles and sensitivity to environmental change (e.g., Hansson & Henttonen, 1988; Sørensen et al., 2023). We implemented a spatial individual-based model that builds on the energy-budget framework in Demonstration 1 but incorporates spatial foraging, movement costs,

digestive dynamics, and tissue-turnover mechanisms appropriate for small mammals.

A full TRACE document, including an ODD protocol (Grimm et al., 2014, 2020; Schmolke et al., 2010), sensitivity analyses, and calibration details, is available as supplemental material. The model code and underlying data are freely available (see Data Accessibility Statement).

Developed in NetLogo v6.2.0 (https://ccl.northwestern.edu/netlogo/), the model simulates interactions between animal agents and a 20x50-cell toroidal landscape. Each 10m×10m cell may contain food resources which replenish over time, with energy content and dry mass informed by vole forage data. The model runs on a 30-minute timestep during the active breeding season (day 90–273), excluding winter due to its relatively limited influence on the processes of focus.

Animals (female adults) are characterized by dynamic state variables tracking morphometrics, energy dynamics, and reproduction. Each timestep involves: (1) movement decisions, (2) energetic costs, (3) resource consumption, and (4) updates to tissue stores, reproduction, and survival.

Movement is represented implicitly: animals “select” a cell within their movement diameter, consume resources from it, and assign a movement speed drawn from a gamma distribution fitted to empirical data. Although positions are not tracked, movement consequences are captured via foraging choice and transport costs, including postural and speed-related components.

Food intake is shaped by energy demand, stomach capacity, hunger, body condition, and local resource availability. Animals attempt to ingest food to offset their energy shortfall, constrained by stomach volume and clearance rates. Digestive capacities adjust dynamically, particularly during lactation, to reflect increased energy needs, consistent with empirical data. Hunger is modeled using dual-intervention theory (Speakman, 2014): increasing at low body fat, decreasing at high body fat, and remaining stable at intermediate levels.

After foraging, animals update their energy balance and adjust tissue stores: surpluses lead to lean and fat deposition, while deficits trigger catabolism. Tissue dynamics follow Forbes' theory (Forbes, 2009), where protein use or deposition increases as body fat decreases, and are grounded in rodent data. Maximum growth rates were set using a subset of exceptionally large animals (Balčiauskienė, 2007). Daily mortality risk, including starvation and abortion, is assessed based on energy stores. Reproduction is triggered by calendar day and reproductive status. At year-end, overwinter mortality occurs and resource levels are reset.

Model calibration

Twelve uncertain parameters were calibrated using POM. Calibration occurred in two stages: (1) resource parameters were adjusted to match empirical bank vole population densities, and (2) sixteen empirical patterns were used to estimate ten sigmoidal allocation parameters governing how body condition influences growth, reproduction, and survival (the eight parameters from Demonstration 1 plus two additional parameters for neonate and offspring mortality).

To ensure realistic abundances, maximum resource levels (g/cell) and accumulation rates (g/timestep) were tested across 25 simulations, with densities compared to several empirical studies (details in TRACE section 6.1.). The best-fitting combination minimized the mean absolute deviation from the median empirical density (14.2 voles/ha).

We again used ABC (van der Vaart et al., 2016) to test 500,000 parameter combinations shaping energy allocation and survival curves. The 30 best-fitting parameter sets were retained (Boult et al., 2018; van der Vaart et al., 2016) to capture greater uncertainty given the increased number of calibration targets.

Model evaluation

After calibration, we assessed the model's ability to replicate the results of an empirical litter manipulation experiment (Koivula et al., 2003), which examined the effects of manipulated litter size on weanling number, body mass, subsequent

breeding attempts, and maternal survival in wild bank voles over three years (1996–1998) in Konnevesi, Finland. Litter manipulation is a classic life-history research method where litter sizes are experimentally altered in females post-birth to explore the costs and trade-offs of reproduction (Koivula et al., 2003; Koskela, 1998; Oksanen et al., 2001).

To mimic the empirical resource environment, the Normalized Difference Vegetation Index (NDVI) (Tucker & Sellers, 1986) was used as a proxy for changes in resource availability. NDVI data were obtained from the extended global NDVI3g product (third generation Global Inventory Modeling and Mapping Studies (GIMMS); Tucker et al., 2005) at bi-weekly resolution for 1990 to 1999 at the study site. This data was accessed using the "gimms" package in R (Detsch, 2023) and interpolated to a daily resolution. A linear relationship between NDVI and food availability was adopted as a pragmatic solution in lieu of empirical data defining these dynamics. NDVI values (0-1) were scaled to a 0–2 modifier for maximum resource levels, where 1 maintained the calibrated value, 0 reduced resources to zero, and 2 was double the calibrated value. Pregnant females were assigned to 'Enlarged' (+2 pups), 'Reduced' (−2 pups), or 'Control' groups. We tracked population abundance and 12 patterns related to birth, weaning, and reproduction (13 patterns total; Table S8.2). To account for stochasticity, we ran 100 simulation replicates spanning the full NDVI forcing period (1990-1999), with model outputs analyzed in R only for the years corresponding to the empirical study.

As a more general evaluation, we compared model outputs to an additional 11 independent empirical patterns (Table S8.1). Outputs from 150 simulations were collected at the end of the fifth simulation year, with further tracking into the sixth year for survival rates. Visual comparisons assessed model agreement with empirical data.

Results

Demonstration 1: Cross-species calibration of energy allocation strategies

Cross-species model calibration

The single-individual energy-budget model successfully reproduced key life-history patterns across six mammal species spanning approximately three orders of magnitude in adult body mass, from *Peromyscus leucopus* (~18 g) to *Procyon lotor* (~6 kg). Across all species, the retained 10 best posterior parameter sets generated close agreement with empirical targets, with simulated values generally falling within ±10–20% of observed trait values (Figure 2A). Posterior uncertainty was modest despite the simplicity of the calibration data, and confidence intervals consistently overlapped empirical values for all five calibration patterns. This indicates that the PIE framework can recover realistic life-history trajectories across wide taxonomic and body-size variation using minimal information.

Emergent allocation strategies with body mass

Posterior parameter sets revealed distinct and biologically interpretable allocation strategies (Figure 2B). Across species, inferred midpoint parameters of allocation curves showed strong and consistent allometric scaling with adult body mass (Figure 2C). Midpoints for growth, pregnancy, and lactation increased with $\log_{10}$ adult mass, with Spearman's rank correlation coefficients of $\rho \approx 0.8$ for growth, $\rho \approx 0.56$ for pregnancy, and $\rho \approx 0.79$ for lactation. These effect sizes indicate that adult body mass explained a substantial fraction of the rank variation in allocation thresholds across species. Consequently, larger species required higher body-fat percentages to initiate somatic growth and reproductive investment and exhibited more conservative allocation strategies, prioritizing maintenance and survival until greater energetic reserves were achieved.

Survival functions displayed particularly steep transitions at low body-fat percentages, reflecting strong selection against starvation. The body-fat thresholds associated with high survival probability also increased with adult body mass

($\rho \approx 0.67$), indicating that larger species experienced elevated starvation risk at comparatively higher absolute fat levels. Together, these relationships are consistent with classic life-history expectations, with fast-paced species reproducing under lower energetic thresholds and slow-paced species requiring greater energetic security, and reflect the generally higher body fat levels characteristic of larger mammals (Calder, 1984; Pitts & Bullard, 1968).

In contrast, steepness parameters exhibited substantially greater posterior variation and weaker associations with adult body mass ($\rho < 0.4$; Figure 2C), indicating that the sensitivity of allocation responses to energetic condition was much less well constrained by the available calibration patterns.

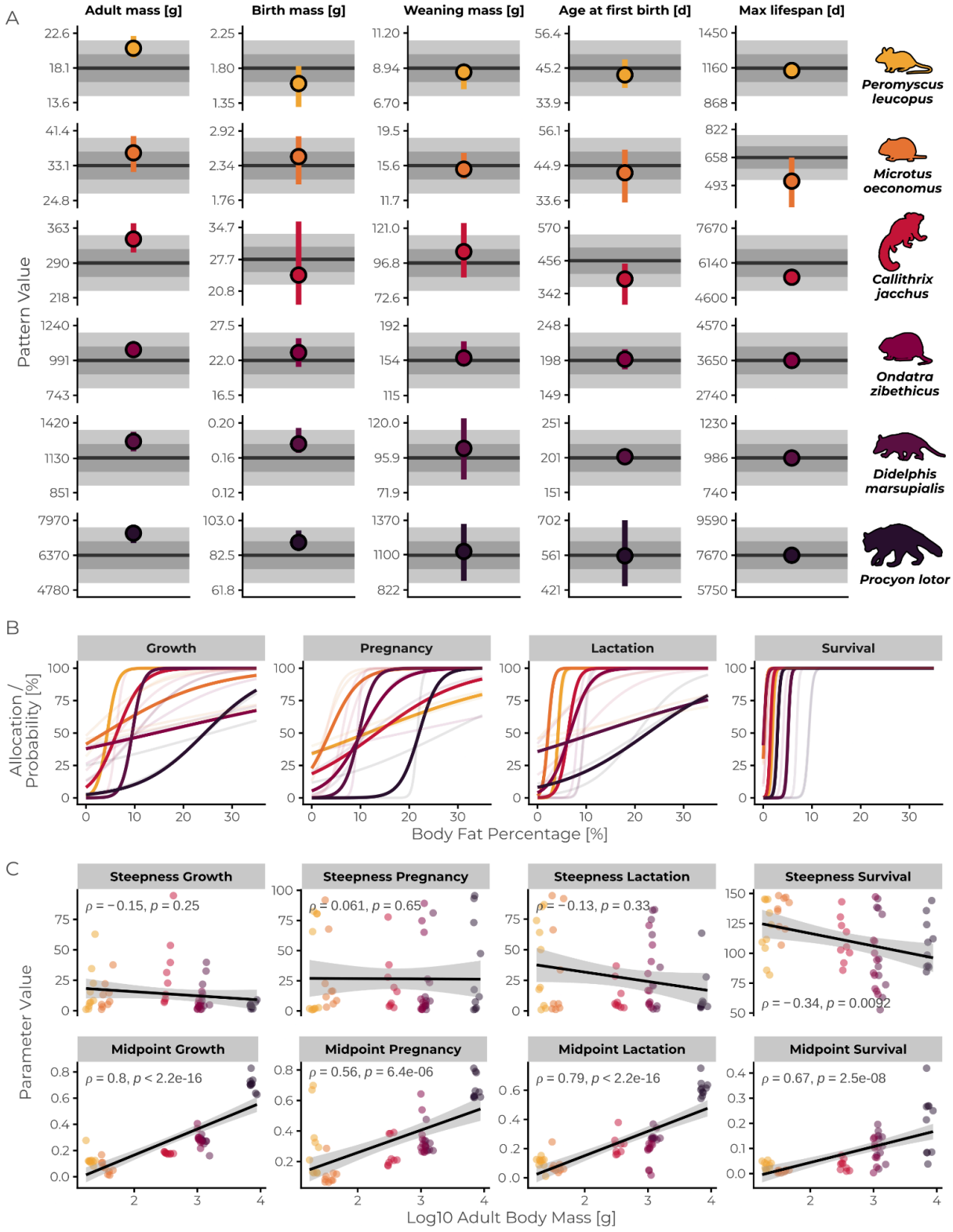
A
Adult mass [g]
Birth mass [g]
Weaning mass [g]
Age at first birth [d]
Max lifespan [d]
Pattern Value
Peromyscus leucopus
Microtus oeconomus
Callithrix jacchus
Ondatra zibethicus
Didelphis marsupialis
Procyon lotor
B
Growth
Pregnancy
Lactation
Survival
Allocation / Probability [%]
Body Fat Percentage [%]
C
Steepness Growth
Steepness Pregnancy
Steepness Lactation
Steepness Survival
ρ = −0.15, p = 0.25
ρ = 0.061, p = 0.65
ρ = −0.13, p = 0.33
ρ = −0.34, p = 0.0092
Midpoint Growth
Midpoint Pregnancy
Midpoint Lactation
Midpoint Survival
ρ = 0.8, p < 2.2e-16
ρ = 0.56, p = 6.4e-06
ρ = 0.79, p < 2.2e-16
ρ = 0.67, p = 2.5e-08
Parameter Value
Log10 Adult Body Mass [g]

Figure 2. Fit of the modelling approach across six mammalian species. (A) Comparison of model predictions for the ten best-fitting parameter sets per species with the empirical patterns used for calibration. Empirical patterns are shown in black, with grey shading indicating ±10% and ±20% deviation around each value, for adult body mass, birth mass, weaning mass, age at first reproduction, and lifespan (left to right) across species. Model outputs show the posterior mean (point) and 50% posterior interval (line). (B) Allocation functions for growth, pregnancy, lactation, and survival probability as functions of body fat percentage, shown for the three best-fitting parameter sets per species, with the top set highlighted in bold. (C) Relationships between log-transformed adult body mass (x-axis) and inferred midpoint or steepness parameters (y-axis) for each allocation function, evaluated across the ten best-fitting parameter sets per species (n = 10 per species; n = 60 total). Points are colored by species. Spearman's rank correlation coefficients (ρ) are shown in grey; black lines indicate linear fits with grey shading showing 95% confidence intervals. Allocation parameters were inferred using Approximate Bayesian Computation applied to 1,000,000 parameter sets per species, with fit assessed via the root sum of squared relative errors. Animal silhouettes are from PhyloPic (phylopic.org) and are in the public domain.

Demonstration 2: Single-Species Validation with Experimental Data

Calibration of population densities, energy allocation, and survival

Calibration of resource dynamics produced realistic population densities, with maximum resource levels of 140 g per grid cell and accumulation rates of 0.011 g per timestep, yielding 14.4 ± 13.7 females per hectare and mid-summer population peaks consistent with empirical observations (empirical mean: 17.5 ± 11.8 females per hectare; TRACE Section 6.1).

Outputs from the 30 best-performing parameter combinations closely matched a diverse set of empirical patterns (Figure 3A–M) (TRACE Section 6.2). Posterior distributions were substantially narrowed, identifying a constrained subset of

parameter values consistent with observed dynamics (TRACE Figure S6.4). In contrast, parameters governing growth and lactation curve steepness showed comparatively weak reduction, though they were more strongly constrained than in Demonstration 1. Discrepancies in predicted mother body mass arise from conflicts between datasets: laboratory studies of lactating females reported higher masses than those used for total adult mass, so the fitted value represents a compromise. Similarly, elevated energy expenditure at very low body masses reflects increased costs under extreme low-condition scenarios, such as intensified foraging to offset declining body condition. Despite these compromises, model outputs remain consistent with observed values and biologically plausible behavior.

The 30 retained parameter combinations were subsequently used in simulations (Figure 3N–P), with variation among runs representing posterior uncertainty in allocation processes.

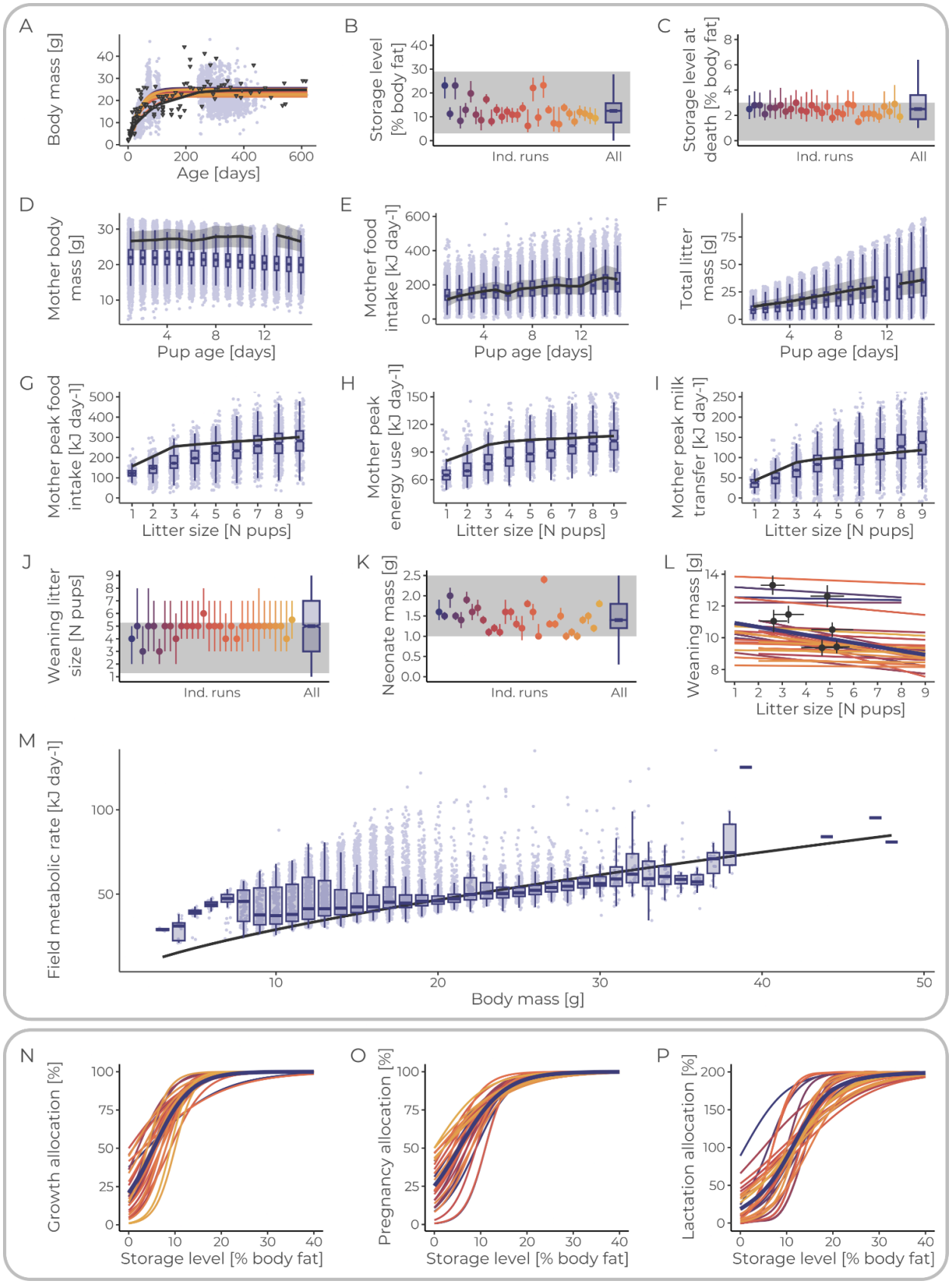
A
Body mass [g]
Age [days]
B
Storage level [% body fat]
Ind. runs
All
C
Storage level at death [% body fat]
Ind. runs
All
D
Mother body mass [g]
Pup age [days]
E
Mother food intake [kJ day-1]
Pup age [days]
F
Total litter mass [g]
Pup age [days]
G
Mother peak food intake [kJ day-1]
Litter size [N pups]
H
Mother peak energy use [kJ day-1]
Litter size [N pups]
I
Mother peak milk transfer [kJ day-1]
Litter size [N pups]
J
Weaning litter size [N pups]
Ind. runs
All
K
Neonate mass [g]
Ind. runs
All
L
Weaning mass [g]
Litter size [N pups]
M
Field metabolic rate [kJ day-1]
Body mass [g]
N
Growth allocation [%]
Storage level [% body fat]
O
Pregnancy allocation [%]
Storage level [% body fat]
P
Lactation allocation [%]
Storage level [% body fat]

Figure 3. Model predictions from the 30 best-fitting parameter combinations are compared with the empirical patterns used for calibration. Panels show: (A) total body mass, (B) percent body fat of living animals, (C) percent body fat at death, (D) mother body mass, (E) food intake, (F) total litter mass with pup age, (G) mother peak food intake, (H) energy use, (I) milk transfer with litter size, (J) litter size at weaning, (K) neonate mass, (L) weanling mass by litter size, and (M) field metabolic rate of non-lactating animals by body mass. Outputs from individual parameter sets appear in unique colors, with combined results shown in purple. Colored point ranges represent the median and 50% CIs for outputs of each parameter set, and light-purple points in panels A, D–I, and M show individual simulation outputs. In panels B–F, J, and K, grey rectangles mark the empirical ranges used to assess fit, while grey shading in D–F represents empirical means ± SE. For panels A, G, H, I, and M, empirical relationships are shown as solid black lines. In panel L, fit was evaluated qualitatively as a negative relationship, with illustrative empirical means ± SE from two studies (Koskela, 1998; Oksanen et al., 2001). In panels A and L, colored lines represent von Bertalanffy or linear fits to model outputs. Panels N–P show the allocation relationships of the 30 best-fitting parameter sets, illustrating how body fat percentage shapes allocation to (N) growth, (O) pregnancy, and (P) lactation. ABC was used to evaluate 500,000 parameter combinations, with fit assessed using median absolute scaled error for zero-variate or multivariate patterns and pass/fail criteria for linear relationships. Additional details and verification patterns are provided in the supplementary TRACE document (Section 6, “Model output verification”).

Replication of a litter manipulation experiment

Model outputs closely matched 13 observed patterns from an independent litter manipulation experiment (Figure 4), providing strong experimental validation across multiple ecological and life-history dimensions. Seasonal population dynamics were accurately reproduced, including characteristic late-summer peaks and interannual differences such as elevated early-summer densities in 1997, although mid-summer values were relatively low in 1996 (Figure 4A).

The model also successfully captured treatment effects on offspring growth. Weanling body mass declined seasonally and was consistently lower in enlarged litters (Figure 4B), demonstrating that the model reproduced how maternal energetic constraints and environmental conditions jointly shape offspring development. Seasonal variation in litter size at weaning was similarly well represented, with the largest litters occurring in mid-summer and smaller litters later in the season (Figure 4C). Female survival patterns aligned closely with observations, including reduced survival in late summer and among females with enlarged litters (Figure 4D), indicating realistic representation of maternal costs.

Despite strong overall agreement, several discrepancies revealed specific limitations of the current model structure. While it correctly predicted smaller weaned litters for reduced litters, it consistently overestimated litter size at weaning and did not reproduce the observed decoupling between birth and weaning litter size, particularly in early and mid-summer. The weaker relationship between birth and weaned litter size observed in late summer, however, was more accurately reproduced, consistent with the reduced variation among manipulation groups later in the season.

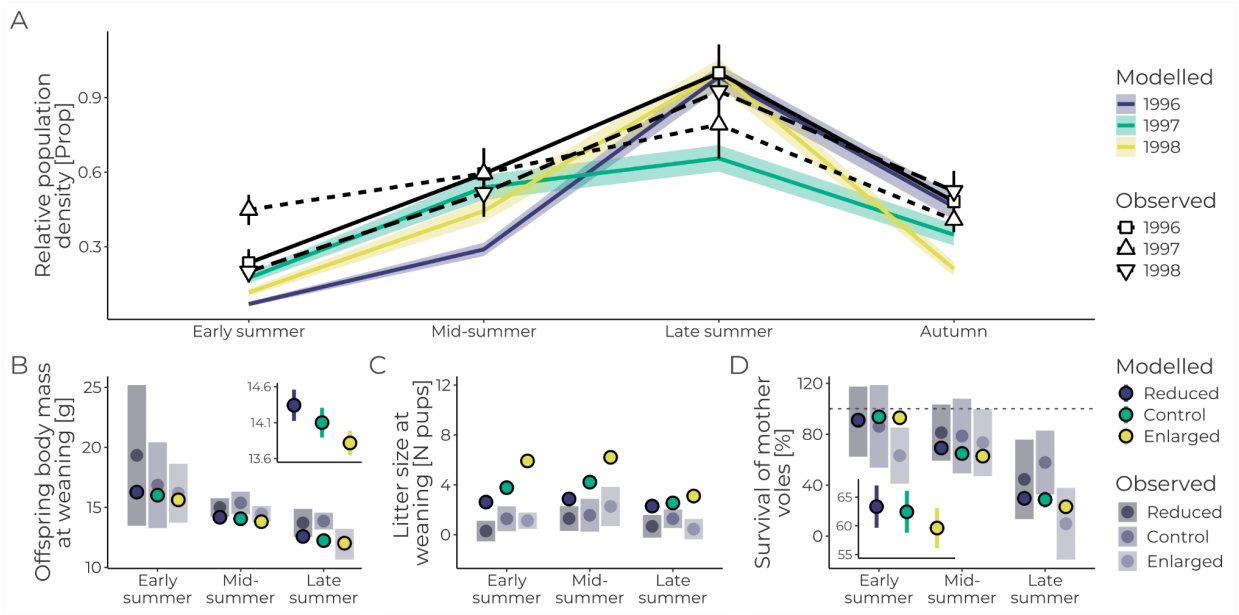

Figure 4. Comparison of model outputs with empirical data from the litter manipulation experiment in Konnevesi, Finland for 1996-1998 (Koivula et al. 2003). (A) Seasonal population density dynamics per year (proportion of maximum value) (mean ± SE), (B) offspring body mass (in grams) at weaning, (C) litter size (count pups) at weaning, and (D) mother survival (%) to the next breeding period (means ± 95% CIs). Insets panels in B and D display averages across the seasons (means ± 95% CIs), with the dotted line in panel D representing 100% survival. Predictions were generated from 100 simulation replicates. All observed estimates were taken directly from plots presented in Koivula et al. (2003).

Broader model evaluation

Model performance was strongly supported by validation against independent datasets on energy dynamics, survival, life history, and morphometrics (TRACE Section 8.1). In particular, field metabolic rates and food consumption across age classes closely matched estimates from nine independent studies (Figure 5), reflecting emergent total energy use and intake from modeled behavior, energetic costs, and allocation strategies. Although some patterns were not fully independent from calibration data (e.g., lactating female intake, though these came from independent studies), others were (e.g., pregnancy and juvenile intake), highlighting that the approach was able to reliably capture diverse energetic and life-history dynamics.

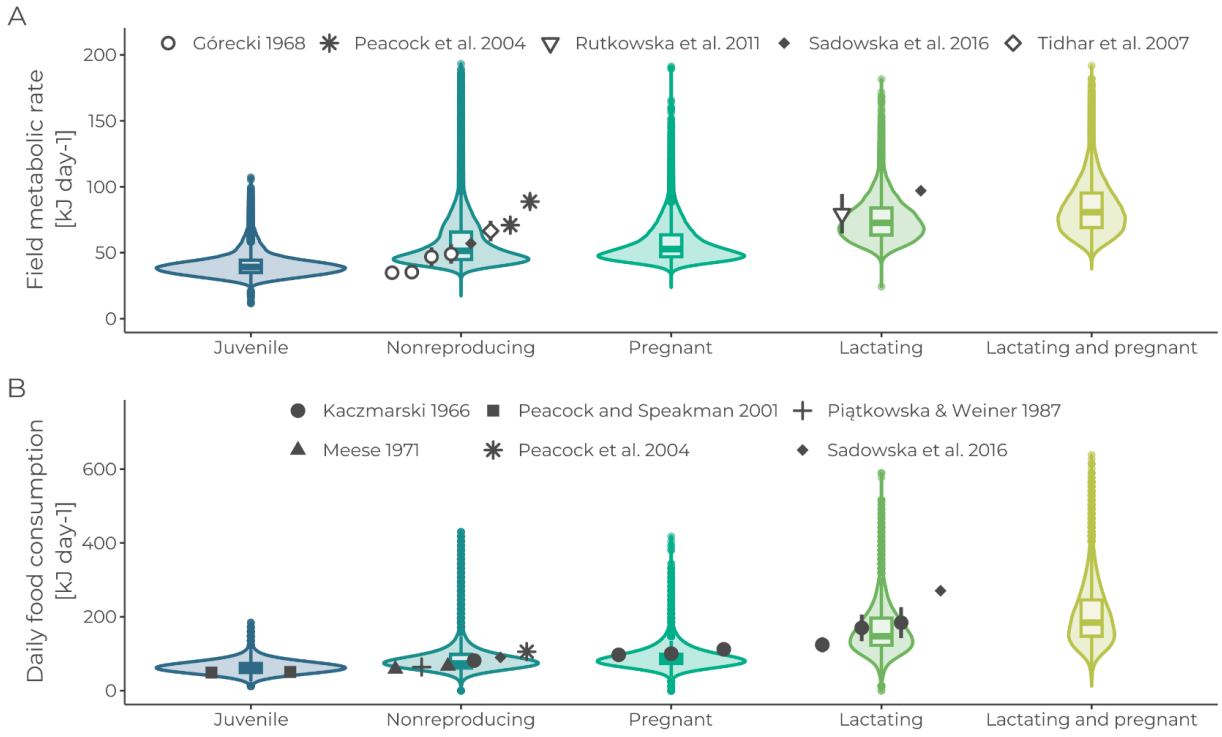

Figure 5. Comparison of model predictions (blue-yellow) with eleven empirical patterns (in grey) for (A) state-dependent field metabolic rates and (B) state-dependent food consumption. Empirical points represent study means, and whiskers show reported error estimates. Model predictions are summarized using violin and box plots; boxes span the interquartile range with the median indicated by a horizontal line, whiskers extend to 1.5× the interquartile range, and points beyond are shown as outliers. Empirical data were unavailable for juvenile, pregnant, and lactating animals in panel A, and for pregnant and lactating animals in panel B, but model outputs for these states are shown for context. Model outputs are presented from 150 simulation replicates.

Discussion

Allocation remains among the most difficult energetic processes to directly measure (McHuron et al., 2022; Sibly et al., 2013). The PIE framework infers allocation dynamics from empirical patterns using inverse parameter estimation, capturing processes that are otherwise unobservable. Rather than prescribing fixed or hierarchical

allocation rules, PIE allows allocation to be species-specific, dynamic, and condition dependent, while explicitly incorporating uncertainty through parameter distributions. By grounding allocation in empirical patterns spanning morphometrics, energetics, life history, and population dynamics, the approach enables mechanistic models to reproduce observed biological variation without relying on ad hoc assumptions, while enabling species-specific deviations that reflect natural variation in life histories.

Across both demonstrations, a cross-species comparison of six mammals and a spatially explicit individual-based model of bank voles, PIE successfully generated realistic allocation strategies, population dynamics, and life-history outcomes, while also revealing which aspects of energy allocation are well constrained by the available data used and which remain weakly identifiable. By highlighting which parameters are strongly informed by empirical patterns and which are not, PIE also serves as a diagnostic tool to identify data gaps and clarify the types of information needed to inform different allocation processes. This not only facilitates model parameterization but also allows researchers to evaluate the inferential limits of existing datasets. Finally, because allocation functions are expressed in terms of energetic condition, PIE generates testable predictions about allocation and population dynamics that can be evaluated with targeted empirical studies.

Key insights from the demonstrations

Across both demonstrations, consistent patterns emerged regarding parameter identifiability. Aggregate empirical patterns strongly constrained allocation thresholds, represented by midpoint parameters of allocation and survival curves. In the cross-species demonstration, midpoint parameters scaled allometrically with body mass, producing biologically interpretable allocation strategies consistent with a slow-fast life-history continuum (Stearns, 1983). Although this analysis included only six species, the emergence of these relationships from energetic constraints alone suggests that allometric scaling in allocation may arise naturally from differences in energetic storage and demand, rather than requiring explicit optimization

assumptions. Broader taxonomic testing will be necessary to evaluate the generality of this result.

In contrast, parameters governing sensitivity to energetic condition (curve steepness) were consistently less identifiable. In the population-level demonstration, steepness parameters were somewhat more constrained than in the cross-species case, reflecting the larger number and diversity of calibration patterns, but they remained difficult to estimate independently. Positive correlations between steepness and corresponding midpoints indicated compensatory relationships, reinforcing that variation in allocation thresholds exerted a stronger influence on model outputs than variation in sensitivity around those thresholds. This weak identifiability likely reflects both data and methodological limitations. Aggregate life-history traits (i.e., zero-variate data such as average adult mass, age at maturity, or lifespan) provide little information on how allocation changes across energetic gradients, and shallow sigmoidal relationships are inherently difficult to distinguish from linear or weakly nonlinear responses when inferred from sparse or aggregated data. Previous work shows that reliably estimating the slope of shallow sigmoids requires dense observations across a wide range of states ; without such coverage, midpoint and slope parameters trade off, leaving sensitivity weakly constrained even when thresholds are well identified. Constraining sensitivity to energetic condition therefore likely requires either explicit consideration of variation within parameter combinations (e.g., using overlap in range of body masses as a pattern) or, more ideally, process-level data such as growth, reproduction, or survival measured across gradients of body condition, resource availability, or energy intake. For instance, recent studies link body condition and mass gain to reproductive performance in species like polar bears (*Ursus maritimus*), badgers (*Meles meles*), and elephant seals (*Mirounga angustirostris*) (L. Archer et al., 2023; Beltran et al., 2023; Bright Ross et al., 2021). These advances provide directly applicable patterns for PIE that offer immense potential for improving the realism and accuracy of bioenergetic models.

Evaluation with independent data and experiments

A central strength of the second demonstration was evaluation against independent empirical data. When applied to a litter manipulation experiment (Koivula et al., 2003), the model reproduced a wide range of observed patterns, including seasonal population dynamics, treatment effects on offspring mass, and maternal survival costs associated with season and enlarged litters. These results demonstrate that allocation strategies inferred through PIE are not merely descriptive, but predictive under novel experimental conditions.

At the same time, model mismatches proved equally informative. The model consistently overestimated litter size at weaning and failed to fully reproduce the empirical decoupling between birth litter size and weaned litter size, particularly early in the breeding season. These discrepancies point to processes affecting offspring survival between birth and weaning that are not fully captured by the current model, such as selective feeding, infanticide, or dispersal (Mazurkiewicz & Rajska, 1975; Sadowska et al., 2016; Ylönen et al., 1997), and are consistent with weakly constrained sensitivity of reproductive allocation to maternal condition. The improved fit later in the season, when empirical differences among manipulation groups were reduced, suggests that seasonal variation in energetic constraints plays an important role. Importantly, these mismatches do not indicate model inadequacy, but instead highlight specific mechanisms and data types needed to explain context-dependent reproductive outcomes.

In this way, PIE facilitates mechanistic interpretation of both successes and failures. Agreement identifies which ecological processes are sufficiently captured by energetic constraints, while mismatches highlight where additional patterns or behavioral or ecological mechanisms may be necessary.

Applying PIE

The PIE framework is most useful in systems where multiple empirical datasets are available across biological levels, such as growth, reproduction, and survival. It is particularly well suited to seasonal or fluctuating environments, or when management or experimental interventions influence intake and expenditure.

Researchers planning to apply PIE should prioritize collecting high-resolution, diverse data that constrain both allocation thresholds and sensitivity to energetic state, as these patterns are essential for reliable inverse inference. Accurate inference of condition-dependent allocation can be especially important in conservation or management contexts, where small differences in allocation thresholds or sensitivity may substantially affect predictions of survival, reproductive output, and population trajectories under environmental stress, harvest, or resource supplementation scenarios. In contrast, for broader ecological or comparative questions, simpler frameworks with fixed or species-constant allocation rules may provide sufficient insight, particularly when high-resolution datasets are unavailable. As with all mechanistic modeling approaches, the framework's complexity should be tailored to the scientific question at hand (Sun et al., 2016).

The demonstrations provide guidance on data requirements for applying PIE. At a minimum (as in Demonstration 1), morphometrics, basic life-history traits, and a modest number of empirical patterns spanning different processes can be sufficient to constrain allocation midpoints. More informative inference (as in Demonstration 2) benefits from population dynamics, energetic measurements, reproductive detail, and independent validation data.

Across applications, several practical principles emerge: prioritize diverse patterns related to each of the parameterized processes over many similar ones; validate model predictions using independent datasets whenever possible; report parameter uncertainty explicitly; and interpret discrepancies mechanistically rather than treating them as model failure.

Limitations and assumptions

The PIE framework relies on several assumptions though. In particular, empirical patterns are treated as reliable representations of system function, yet real datasets often contain substantial epistemic uncertainties, arising from measurement error, sampling bias, model structural limitations, and study design choices, that are not well captured by purely aleatory error models. Additionally many calibration

variables, such as adult body mass, mother body mass, food intake, energy expenditure, and litter size, are intrinsically correlated, effectively reducing the number of independent constraints and inflating the apparent information content of the dataset. When such epistemic uncertainties or correlations are ignored or mis-specified, parameter inference can become over-conditioned, producing an artificially narrow parameter space (Beven & Binley, 2014; Gallagher, Chudzinska, et al., 2021). Using multiple, independent patterns can mitigate these effects (Grimm, 2005), and virtual ecologist approaches may further reduce bias (Zurell et al., 2010). Future applications could explicitly assess the effective dimensionality of calibration data, for example through analyses of pairwise correlations or more formal characterizations of the geometry of the parameter space (Radchuk et al., 2019), to guide the selection of patterns that maximize independent information.

In real systems, allocation relationships can also change with age or differ among individuals (Glazier, 2008). Age-dependent shifts could be incorporated by parameterizing allocation curves separately for different life stages when such data exist, whereas individual-level variation could be represented by assigning parameter values to each simulated individual rather than applying a single population-level curve to each simulation.

Patterns themselves are also treated as static, despite the potential for plasticity, adaptation, and evolution to shift relationships over time (Edelaar & Bolnick, 2019). For long-term forecasts, incorporating adaptive dynamics may be necessary (Wortel et al., 2023). In addition, inference depends on model structure: incorrect mechanistic assumptions will yield misleading parameter estimates. Testing alternative energetic formulations remains an important avenue for future work.

Finally, inverse parameter estimation can be computationally demanding for complex models. Efficient sampling strategies, hierarchical calibration, and parallelization can reduce these costs, but methods that preserve uncertainty in allocation processes remain essential.

Comparison to alternative approaches

Unlike optimization-based models (Mangel, 2015; McNamara & Houston, 1996), PIE does not assume allocation strategies are fitness-optimal, instead deriving them directly from observed outcomes, an advantage when optimality is uncertain or selection pressures are unclear. Compared to Dynamic Energy Budget models (Kooijman, 2000; Nisbet et al., 2000), which assume fixed allocation fractions (κ) that work well for many applications, PIE provides greater flexibility for representing condition-dependent allocation shifts, though with fewer a priori theoretical constraints and potentially more free parameters. Fixed hierarchical allocation schemes (Sibly et al., 2013) may prioritize maintenance over reproduction over growth in clear sequences, simplifying implementation, but cannot capture simultaneous, condition-dependent reductions across multiple functions. For example, under moderate energy deficit, animals may reduce both growth and reproduction rather than completely sacrificing one for the other (Parker et al., 2009), a dynamic PIE represents naturally through independent allocation curves that respond to the same physiological state. Importantly, while other frameworks have used similar sigmoidal or condition-dependent allocation relationships (e.g., Archer et al., 2025; Gallagher et al., 2021; Hin et al., 2019), these have rarely been directly informed by empirical data.

Cross-species PIE analyses enable empirical adjudication among competing allocation frameworks by comparing the inferred, condition-dependent allocation patterns to theory-specific predictions, for example, DEB's κ-fraction constancy, hierarchical triage that suppresses growth/reproduction under deficits, or optimality-based strategies, thus revealing which theoretical rules may be most consistent with the data in different taxa or environmental contexts.

Importantly, PIE principles can be integrated into existing frameworks by making allocation parameters condition-dependent rather than fixed, highlighting complementarity rather than competition among approaches. Additionally, while we demonstrate PIE with mammalian pregnancy and lactation, the approach transfers readily to other systems, allocation curves could govern egg production, parental provisioning, or fertility in birds, fish, or invertebrates, provided relevant empirical patterns exist to constrain parameters.

Conclusion

The PIE framework offers a data-driven alternative to assumption-based energy allocation in mechanistic models. By integrating empirical patterns through inverse parameter estimation, it enables dynamic allocation, explicitly represents uncertainty, and reveals both the strengths and limits of available data. Across two demonstrations spanning cross-species and within-population scales, PIE successfully reproduced a broad suite of ecological patterns and validated predictions against independent experimental data.

Equally important, the framework clarifies what cannot be learned from existing information, identifying when additional data or mechanisms are required. In doing so, PIE advances predictive ecology by grounding allocation dynamics in empirical reality while remaining transparent about uncertainty, assumptions, and inference limits. As empirical datasets linking energetics, condition, and fitness continue to expand, PIE provides a flexible and extensible approach for integrating this information into mechanistic ecological models.

References

Archer, L., Atkinson, S., Pagano, A., Penk, S., & Molnár, P. (2023). Lactation performance in polar bears is associated with fasting time and energetic state. *Marine Ecology Progress Series*, *720*, 175–189. https://doi.org/10.3354/meps14382

Archer, L. C., Atkinson, S. N., Lunn, N. J., Penk, S. R., & Molnár, P. K. (2025). Energetic constraints drive the decline of a sentinel polar bear population. *Science*, *387*(6733), 516–521. https://doi.org/10.1126/science.adp3752

Balčiauskienė, L. (2007). Cranial growth of captive bred bank voles (*Clethrionomys glareolus*). *Acta Zoologica Lituanica*, *17*(1), 33–40. https://doi.org/10.1080/13921657.2007.10512813

Beltran, R. S., Hernandez, K. M., Condit, R., Robinson, P. W., Crocker, D. E., Goetsch, C., Kilpatrick, A. M., & Costa, D. P. (2023). Physiological tipping points in the relationship between

foraging success and lifetime fitness of a long-lived mammal. *Ecology Letters*, *26*(5), 706–716. https://doi.org/10.1111/ele.14193

Beven, K., & Binley, A. (2014). GLUE: 20 years on. *Hydrological Processes*, *28*(24), 5897–5918. https://doi.org/10.1002/hyp.10082

Boult, V. L., Fishlock, V., Quaife, T., Hawkins, E., Moss, C., Lee, P. C., & Sibly, R. M. (2019). Human-driven habitat conversion is a more immediate threat to Amboseli elephants than climate change. *Conservation Science and Practice*, *1*(9). https://doi.org/10.1111/csp2.87

Boult, V. L., Quaife, T., Fishlock, V., Moss, C. J., Lee, P. C., & Sibly, R. M. (2018). Individual-based modelling of elephant population dynamics using remote sensing to estimate food availability. *Ecological Modelling*, *387*, 187–195. https://doi.org/10.1016/j.ecolmodel.2018.09.010

Boyd, R., Roy, S., Sibly, R., Thorpe, R., & Hyder, K. (2018). A general approach to incorporating spatial and temporal variation in individual-based models of fish populations with application to Atlantic mackerel. *Ecological Modelling*, *382*, 9–17. https://doi.org/10.1016/j.ecolmodel.2018.04.015

Bright Ross, J. G., Newman, C., Buesching, C. D., Connolly, E., Nakagawa, S., & Macdonald, D. W. (2021). A fat chance of survival: Body condition provides life-history dependent buffering of environmental change in a wild mammal population. *Climate Change Ecology*, *2*, 100022. https://doi.org/10.1016/j.ecochg.2021.100022

Calder, W. A. (1984). *Size, Function, and Life History*. Harvard University Press.

Christiansen, F., Víkingsson, G. A., Rasmussen, M. H., & Lusseau, D. (2014). Female body condition affects foetal growth in a capital breeding mysticete. *Functional Ecology*, *28*(3), 579–588. https://doi.org/10.1111/1365-2435.12200

Clairbaux, M., Mathewson, P., Porter, W., Fort, J., Strøm, H., Moe, B., Fauchald, P., Descamps, S., Helgason, H. H., & Bråthen, V. S. (2021). North Atlantic winter cyclones starve seabirds. *Current Biology: CB*, *31*(17), 3964–3971.

Detsch, F. (2023). *gimms: Download and Process GIMMS NDVI3g Data* (Version 1.2.2) [Computer software]. https://cran.r-project.org/web/packages/gimms/index.html

Edelaar, P., & Bolnick, D. I. (2019). Appreciating the Multiple Processes Increasing Individual or Population Fitness. *Trends in Ecology & Evolution*, *34*(5), 435–446. https://doi.org/10.1016/j.tree.2019.02.001

Forbes, G. B. (2009). Lean Body Mass-Body Fat Interrelationships in Humans. *Nutrition Reviews*, *45*(10), 225–231. https://doi.org/10.1111/j.1753-4887.1987.tb02684.x

Gallagher, C. A., Chudzinska, M., Larsen-Gray, A., Pollock, C. J., Sells, S. N., White, P. J. C., & Berger, U. (2021). From theory to practice in pattern-oriented modelling: Identifying and using empirical patterns in predictive models. *Biological Reviews*, *96*(5), 1868–1888. https://doi.org/10.1111/brv.12729

Gallagher, C. A., Grimm, V., Kyhn, L. A., Kinze, C. Chr., & Nabe-Nielsen, J. (2021). Movement and seasonal energetics mediate vulnerability to disturbance in marine mammal populations. *The American Naturalist*, *197*(3), 296–311. https://doi.org/10.1086/712798

Gittleman, J. L., & Thompson, S. D. (1988). Energy Allocation in Mammalian Reproduction. *American Zoologist*, *28*(3), 863–875. https://doi.org/10.1093/icb/28.3.863

Glazier, D. S. (2008). Resource allocation patterns. In W. M. Rauw (Ed.), *Resource allocation theory applied to farm animal production* (1st ed., pp. 22–43). CABI. https://doi.org/10.1079/9781845933944.0022

Grimm, V. (2005). Pattern-Oriented Modeling of Agent-Based Complex Systems: Lessons from Ecology. *Science*, *310*(5750), 987–991. https://doi.org/10.1126/science.1116681

Grimm, V., Augusiak, J., Focks, A., Frank, B. M., Gabsi, F., Johnston, A. S. A., Liu, C., Martin, B. T., Meli, M., Radchuk, V., Thorbek, P., & Railsback, S. F. (2014). Towards better modelling and decision support: Documenting model development, testing, and analysis using TRACE. *Ecological Modelling*, *280*, 129–139. https://doi.org/10.1016/j.ecolmodel.2014.01.018

Grimm, V., & Railsback, S. F. (2012). Pattern-oriented modelling: A 'multi-scope' for predictive systems ecology. *Philosophical Transactions of the Royal Society B: Biological Sciences*, *367*(1586), 298–310. https://doi.org/10.1098/rstb.2011.0180

Grimm, V., Railsback, S. F., Vincenot, C. E., Berger, U., Gallagher, C., DeAngelis, D. L., Edmonds, B., Ge, J., Giske, J., Groeneveld, J., Johnston, A. S. A., Milles, A., Nabe-Nielsen, J., Polhill, J. G., Radchuk, V., Rohwäder, M.-S., Stillman, R. A., Thiele, J. C., & Ayllón, D. (2020). The ODD Protocol for Describing Agent-Based and Other Simulation Models: A Second Update to Improve Clarity, Replication, and Structural Realism. *Journal of Artificial Societies and Social Simulation*, *23*(2), 7. https://doi.org/10.18564/jasss.4259

Hansson, L., & Henttonen, H. (1988). Rodent dynamics as community processes. *Trends in Ecology & Evolution*, *3*(8), 195–200. https://doi.org/10.1016/0169-5347(88)90006-7

Hartig, F., Calabrese, J. M., Reineking, B., Wiegand, T., & Huth, A. (2011). Statistical inference for stochastic simulation models - theory and application: Inference for stochastic simulation models. *Ecology Letters*, *14*(8), 816–827. https://doi.org/10.1111/j.1461-0248.2011.01640.x

Hin, V., Harwood, J., & de Roos, A. M. (2019). Bio-energetic modeling of medium-sized cetaceans shows high sensitivity to disturbance in seasons of low resource supply. *Ecological Applications*, *29*(5), e01903. https://doi.org/10.1002/eap.1903

Jones, K. E., Bielby, J., Cardillo, M., Fritz, S. A., O'Dell, J., Orme, C. D. L., Safi, K., Sechrest, W., Boakes, E. H., Carbone, C., Connolly, C., Cutts, M. J., Foster, J. K., Grenyer, R., Habib, M., Plaster, C. A., Price, S. A., Rigby, E. A., Rist, J., … Purvis, A. (2009). PanTHERIA: A species-level database of life history, ecology, and geography of extant and recently extinct mammals. *Ecology*, *90*(9), 2648–2648. https://doi.org/10.1890/08-1494.1

Koivula, M., Koskela, E., Mappes, T., & Oksanen, T. A. (2003). Cost of reproduction in the wild: Manipulation of reproductive effort in the bank vole. *Ecology*, *84*(2), 398–405. https://doi.org/10.1890/0012-9658(2003)084%255B0398:CORITW%255D2.0.CO;2

Kooijman, S. A. L. M. (2000). *Dynamic Energy and Mass Budgets in Biological Systems*. Cambridge University Press.

Koskela, E. (1998). Offspring growth, survival and reproductive success in the bank vole: A litter size manipulation experiment. *Oecologia*, *115*(3), 379–384. https://doi.org/10.1007/s004420050531

Lamb, S., McMillan, B. R., van de Kerk, M., Frandsen, P. B., Hersey, K. R., & Larsen, R. T. (2023). From conception to recruitment: Nutritional condition of the dam dictates the likelihood of success in a temperate ungulate. *Frontiers in Ecology and Evolution*, *11*. https://doi.org/10.3389/fevo.2023.1090116

Mangel, M. (2015). Stochastic Dynamic Programming Illuminates the Link Between Environment, Physiology, and Evolution. *Bulletin of Mathematical Biology*, *77*(5), 857–877. https://doi.org/10.1007/s11538-014-9973-3

Mazurkiewicz, M., & Rajska, E. (1975). Dispersion of young bank voles from their place of birth. *Acta Theriologica*, *20*, 71–81. https://doi.org/10.4098/AT.arch.75-6

McHuron, E. A., Adamczak, S., Arnould, J. P. Y., Ashe, E., Booth, C., Bowen, W. D., Christiansen, F., Chudzinska, M., Costa, D. P., Fahlman, A., Farmer, N. A., Fortune, S. M. E., Gallagher, C. A., Keen, K. A., Madsen, P. T., McMahon, C. R., Nabe-Nielsen, J., Noren, D. P., Noren, S. R., … Williams, R. (2022). Key questions in marine mammal bioenergetics. *Conservation Physiology*, *10*(1), coac055. https://doi.org/10.1093/conphys/coac055

McKay, M. D. (1992). Latin hypercube sampling as a tool in uncertainty analysis of computer models. *Proceedings of the 24th Conference on Winter Simulation - WSC '92*, 557–564. https://doi.org/10.1145/167293.167637

McNamara, J. M., & Houston, A. I. (1996). State-dependent life histories. *Nature*, *380*(6571), Article 6571. https://doi.org/10.1038/380215a0

Nisbet, R. M., Muller, E. B., Lika, K., & Kooijman, S. (2000). From molecules to ecosystems through dynamic energy budget models. *Journal of Animal Ecology*, 913–926.

Oksanen, T. A., Jonsson, P., Koskela, E., & Mappes, T. (2001). Optimal allocation of reproductive effort: Manipulation of offspring number and size in the bank vole. *Proceedings of the Royal Society of London. Series B: Biological Sciences*, *268*(1467), 661–666. https://doi.org/10.1098/rspb.2000.1409

Parker, K. L., Barboza, P. S., & Gillingham, M. P. (2009). Nutrition integrates environmental responses of ungulates. *Functional Ecology*, *23*(1), 57–69. https://doi.org/10.1111/j.1365-2435.2009.01528.x

Pitts, G. C., & Bullard, T. R. (1968). Some interspecific aspects of body composition in mammals. In *Body composition in animals and man* (Vol. 45, p. 70). National Academy of Science Washington, District of Columbia.

Pontzer, H., & McGrosky, A. (2022). Balancing growth, reproduction, maintenance, and activity in evolved energy economies. *Current Biology*, *32*(12), R709–R719. https://doi.org/10.1016/j.cub.2022.05.018

R Core Team. (2024). *R: A language and environment for statistical computing* [Computer software]. R Foundation for Statistical Computing. https://www.R-project.org/

Radchuk, V., Laender, F. D., Cabral, J. S., Boulangeat, I., Crawford, M., Bohn, F., Raedt, J. D., Scherer, C., Svenning, J.-C., Thonicke, K., Schurr, F. M., Grimm, V., & Kramer-Schadt, S. (2019). The Dimensionality of Stability Depends on Disturbance Type. *Ecology Letters*, *22*(4), 674–684. https://doi.org/10.1111/ele.13226

Ricklefs, R. E. (2010). Embryo growth rates in birds and mammals. *Functional Ecology*, *24*(3), 588–596. https://doi.org/10.1111/j.1365-2435.2009.01684.x

Ricklefs, R. E., & Wikelski, M. (2002). The physiology/life-history nexus. *Trends in Ecology & Evolution*, *17*(10), 462–468. https://doi.org/10.1016/S0169-5347(02)02578-8

Sadowska, E. T., Król, E., Chrzascik, K. M., Rudolf, A. M., Speakman, J. R., & Koteja, P. (2016). Limits to sustained energy intake. XXIII. Does heat dissipation capacity limit the energy budget of lactating bank voles? *Journal of Experimental Biology*, jeb.134437. https://doi.org/10.1242/jeb.134437

Schmolke, A., Thorbek, P., DeAngelis, D. L., & Grimm, V. (2010). Ecological models supporting environmental decision making: A strategy for the future. *Trends in Ecology & Evolution*, *25*(8), 479–486. https://doi.org/10.1016/j.tree.2010.05.001

Sibly, R. M., Grimm, V., Martin, B. T., Johnston, A. S. A., Kułakowska, K., Topping, C. J., Calow, P., Nabe-Nielsen, J., Thorbek, P., & DeAngelis, D. L. (2013). Representing the acquisition and use of energy by individuals in agent-based models of animal populations. *Methods in Ecology and Evolution*, *4*(2), 151–161. https://doi.org/10.1111/2041-210x.12002

Sørensen, O. J., Moa, P. F., Hagen, B.-R., & Selås, V. (2023). Possible impact of winter conditions and summer temperature on bank vole (*Myodes glareolus*) population fluctuations in Central Norway. *Ethology Ecology & Evolution*, *35*(4), 471–487. https://doi.org/10.1080/03949370.2022.2120084

Speakman, J. R. (2014). If Body Fatness is Under Physiological Regulation, Then How Come We Have an Obesity Epidemic? *Physiology*, *29*(2), 88–98. https://doi.org/10.1152/physiol.00053.2013

Stearns, S. C. (1983). The Influence of Size and Phylogeny on Patterns of Covariation among Life-History Traits in the Mammals. *Oikos*, *41*(2), 173. https://doi.org/10.2307/3544261

Stephenson, T. R., German, D. W., Cassirer, E. F., Walsh, D. P., Blum, M. E., Cox, M., Stewart, K. M., & Monteith, K. L. (2020). Linking population performance to nutritional condition in an alpine ungulate. *Journal of Mammalogy*, *101*(5), 1244–1256. https://doi.org/10.1093/jmammal/gyaa091

Sun, Z., Lorscheid, I., Millington, J. D., Lauf, S., Magliocca, N. R., Groeneveld, J., Balbi, S., Nolzen, H., Müller, B., Schulze, J., & Buchmann, C. M. (2016). Simple or complicated agent-based models? A complicated issue. *Environmental Modelling & Software*, *86*, 56–67. https://doi.org/10.1016/j.envsoft.2016.09.006

Tollefson, T. N., Shipley, L. A., Myers, W. L., Keisler, D. H., & Dasgupta, N. (2010). Influence of Summer and Autumn Nutrition on Body Condition and Reproduction in Lactating

Mule Deer. *The Journal of Wildlife Management*, *74*(5), 974–986. https://doi.org/10.2193/2008-529

Tucker, C. J., Pinzon, J. E., Brown, M. E., Slayback, D. A., Pak, E. W., Mahoney, R., Vermote, E. F., & El Saleous, N. (2005). An extended AVHRR 8-km NDVI dataset compatible with MODIS and SPOT vegetation NDVI data. *International Journal of Remote Sensing*, *26*(20), 4485–4498. https://doi.org/10.1080/01431160500168686

Tucker, C. J., & Sellers, P. J. (1986). Satellite remote sensing of primary production. *International Journal of Remote Sensing*, *7*(11), 1395–1416. https://doi.org/10.1080/01431168608948944

Van Benthem, K. J., Froy, H., Coulson, T., Getz, L. L., Oli, M. K., & Ozgul, A. (2017). Trait–demography relationships underlying small mammal population fluctuations. *Journal of Animal Ecology*, *86*(2), 348–358. https://doi.org/10.1111/1365-2656.12627

van der Vaart, E., Johnston, A. S. A., & Sibly, R. M. (2016). Predicting how many animals will be where: How to build, calibrate and evaluate individual-based models. *Ecological Modelling*, *326*, 113–123. https://doi.org/10.1016/j.ecolmodel.2015.08.012

van der Vaart, E., Prangle, D., & Sibly, R. M. (2018). Taking error into account when fitting models using Approximate Bayesian Computation. *Ecological Applications*, *28*(2), 267–274. https://doi.org/10.1002/eap.1656

White, C. R., Alton, L. A., Bywater, C. L., Lombardi, E. J., & Marshall, D. J. (2022). Metabolic scaling is the product of life-history optimization. *Science*, *377*(6608), 834–839. https://doi.org/10.1126/science.abm7649

Winberg, G. G. (1956). Rate of metabolism and food requirements of fishes. *Fish. Res. Bd. Canada Trans. Ser.*, *433*, 1–251.

Wortel, M. T., Agashe, D., Bailey, S. F., Bank, C., Bisschop, K., Blankers, T., Cairns, J., Colizzi, E. S., Cusseddu, D., Desai, M. M., van Dijk, B., Egas, M., Ellers, J., Groot, A. T., Heckel, D. G., Johnson, M. L., Kraaijeveld, K., Krug, J., Laan, L., … Pennings, P. S. (2023). Towards evolutionary predictions: Current promises and challenges. *Evolutionary Applications*, *16*(1), 3–21. https://doi.org/10.1111/eva.13513

Ylönen, H., Koskela, E., & Mappes, T. (1997). Infanticide in the bank vole (*Clethrionomys glareolus*): Occurrence and the effect of familiarity on female infanticide. *Annales Zoologici Fennici*, 259–266. https://www.jstor.org/stable/23735490

Zullinger, E. M., Ricklefs, R. E., Redford, K. H., & Mace, G. M. (1984). Fitting sigmoidal equations to mammalian growth curves. *Journal of Mammalogy*, *65*(4), 607–636.

Zurell, D., Berger, U., Cabral, J. S., Jeltsch, F., Meynard, C. N., Münkemüller, T., Nehrbass, N., Pagel, J., Reineking, B., Schröder, B., & Grimm, V. (2010). The virtual ecologist approach: Simulating data and observers. *Oikos*, *119*(4), 622–635. https://doi.org/10.1111/j.1600-0706.2009.18284.x

Appendix tables:

Table S1. State variables used in the model.

Code name	Description [units]	Symbol	Type
structural_mass	Structural (fat-free) body mass [g]	m_{LM}	float
fat_mass	Stored fat mass [g]	m_{adi}	float
storage_level	Body fat proportion [proportion, 0–1]	SL	float
emb_mass	Embryo mass [g]	m_{emb}	float
off_mass	Offspring mass per offspring during lactation [g]	m_{off}	float
age	Individual age [days]	age	integer
state	Reproductive/survival state: "resting", "pregnant", "lactating", "dead" [unitless]	$state$	string

days_in_state	Days elapsed in current reproductive state [days]	ds	integer
days_since_last_birth	Days since last birth event (reset on birth) [days]	ds_{birth}	integer
survival_prob	Daily survival probability given fat state [probability, 0–1]	β_A	float
energy_intake	Total realized daily intake [kJ/day]	IR_{real}	float
energy_balance	Daily energy balance after demands (positive surplus, negative deficit) [kJ/day]	EB	float
maintenance	Daily maintenance expenditure (BMR + foraging costs) [kJ/day]	M_B	float
growth_cost	Total lean mass growth cost [kJ/day]	M_{lm}	float
pregnancy_cost	Total pregnancy cost (embryo synthesis + gestation maintenance increment) [kJ/day]	M_P	float
lactation_cost	Total lactation cost (offspring growth + offspring maintenance) [kJ/day]	M_L	float

Table S2. Parameter definitions and values.

Code	Value	Description [& units]	Symbol	Source
metabolic_rate_constant	computed from PanTHERIA BMR	Normalization constant for maintenance metabolism [kJ/day · g^-metabolic_exponent]	B_0	PanTHERIA (traits)
metabolic_exponent	0.75	Metabolic scaling exponent for maintenance [-]	γ	Sibly et al. 2013
net_assimilation_efficiency	0.8	Fraction of ingested energy available after digestive/assimilation losses [-]	AE	Assumption
foraging_overhead	0.1	Fractional overhead cost for foraging losses applied to intake [-]	FE	Assumption

max_structural_mass	computed (= AdultBodyMass_g × 1.15)	Maximum structural (fat-free) mass [g]	$m_{lm,max}$	PanTHERIA adult mass
energy_per_gram_tissue	7	Energy cost per gram of tissue synthesis [kJ/g]	ED_m	Sibly et al. 2013
tissue_synthesis_efficiency	0.5	Efficiency of converting allocated energy into tissue [-]	DE_m	Sibly et al. 2013
mass_at_maturity	computed	Structural mass threshold for first reproduction [g]	m_{mat}	Derived from Gompertz maturity mass (below)
gompertz_k_growth	computed	Gompertz growth rate parameter for structural growth [1/day]	k	Derived; Zullinger et al. 1984 used to initialize k in fitting
pregnancy_duration	round(GestationLen_d)	Gestation length [days]	t_{gest}	PanTHERIA gestation length
lactation_duration	round(WeaningAge_d)	Lactation/weaning period [days]	t_{nurs}	PanTHERIA weaning age
min_wait_after_birth	round(InterbirthInterval_d − GestationLen_d)	Minimum wait after birth before next pregnancy [days]	t_{wait}	PanTHERIA intervals
gompertz_k_emb	computed (=exp(0.627)* pregnancy_duration ^ -0.905)	Embryo growth Gompertz rate parameter [1/day]	k_{emb}	Ricklefs 2010
gompertz_A_emb	(NeonateBodyMass_g × 2.4)	Embryo asymptotic mass [g]	A_{emb}	Ricklefs 2010
initial_emb_mass	NeonateBodyMass_g × 0.01	Starting embryo mass [g]	$m_{emb,0}$	Assumption
litter_size	round(LitterSize)	Number of offspring per litter [count]	n_{off}	PanTHERIA litter size
energy_per_gram_fat	39.3 × 0.8 (= 31.44)	Energy density of stored fat tissue [kJ/g]	ED_{fat}	Schmidt-Nielsen 1997, adjusted for 80% lipid content (assumed)

fat_storage_efficiency	0.73	Efficiency of converting surplus energy to stored fat [-]	ε_{fat}	Pullar & Webster 1977
fat_mobilization_efficiency	0.8	Efficiency factor applied when mobilizing fat [-]	η_{fat}	Assumption
max_storage_level	35	Maximum sustainable fat percent [%]	SL_{max}	Assumption
target_storage_level	species-specific mean body-fat (SD = 5%)	Target body fat proportion used in intake adjustment [-]	SL_{*}	Pitts and Bullard 1968
steepness_grow	species-specific	Logistic steepness for growth allocation curve [-]	k_{lm}	Calibrated
midpoint_grow	species-specific	Logistic midpoint for growth curve [proportion of max_storage_level]	$x_{0,lm}$	Calibrated
steepness_preg	species-specific	Logistic steepness for pregnancy allocation curve [-]	k_P	Calibrated
midpoint_preg	species-specific	Logistic midpoint for pregnancy curve [proportion of max_storage_level]	$x_{0,P}$	Calibrated
steepness_lact	species-specific	Logistic steepness for lactation allocation curve [-]	k_L	Calibrated
midpoint_lact	species-specific	Logistic midpoint for lactation curve [proportion of max_storage_level]	$x_{0,L}$	Calibrated
steepness_survive	species-specific	Logistic steepness for survival curve [-]	k_S	Calibrated
midpoint_survive	species-specific	Logistic midpoint for survival curve [proportion of max_storage_level]	$x_{0,S}$	Calibrated

Table S3. Model equations.

Eq.	Process	Code	Equation
B1	Basal maintenance	maintenance_cost_BMR	$M_B = B_0 m_{lm}^{\gamma}$
B2	Growth allocation curve [–]	growth_allocation_percent	$a_{lm} = \frac{1}{1 + e^{-k_{lm}(\frac{SL}{SL_{max}} - x_{0,lm})}}$
B3	Maximum somatic growth rate	max_growth_rate	$\dot{m}_{lm} = k \cdot a_{lm} \cdot m_{lm} \ln\left(\frac{m_{lm,max} \cdot a_{lm}}{m_{lm}}\right)$
B4	Somatic growth cost	growth_cost	$M_{lm} = \frac{\dot{m}_{lm} ED_m}{DE_m}$
B5	Pregnancy allocation curve [–]	pregnancy_allocation_percent	$a_P = \frac{1}{1 + e^{-k_P(\frac{SL}{SL_{max}} - x_{0,P})}}$
B6	Embryonic growth rate	daily_growth_rate	$\dot{m}_{emb} = k_{emb} \cdot a_P \cdot m_{emb} \ln\left(\frac{A_{emb} \cdot a_P}{m_{emb}}\right)$
B7	Embryonic growth cost	emb_growth_cost	$M_{lm,emb} = \frac{\dot{m}_{emb} \cdot ED_m}{DE_m} n_{off}$
B8	Gestational overhead	gest_costs	$M_G = B_0(m_{lm} + (m_{emb} \cdot n_{off}))^{\gamma} - M_B$
B9	Pregnancy cost	pregnancy_cost	$M_P = (M_{lm,emb} + M_G) \cdot a_P$
B10	Lactation allocation curve [–]	lactation_allocation_percent	$a_L = \frac{1}{1 + e^{-k_L(\frac{SL}{SL_{max}} - x_{0,L})}}$

B11	Offspring growth rate	off_growth	$\dot{m}_{off} = k \cdot a_L \cdot m_{off} \ln\left(\frac{m_{lm,max} \cdot a_L}{m_{off}}\right)$
B12	Offspring growth cost	off_growth_cost	$M_{lm,off} = \frac{\dot{m}_{off} \cdot ED_m}{DE_m} \cdot n_{off}$
B13	Offspring maintenance	off_maintenance_costs	$M_{B,off} = B_0 m_{off}^{\gamma} \cdot n_{off}$
B14	Lactation allocation curve [–]	lactation_allocation_percent	$a_L = \frac{1}{1 + e^{-k_L(\frac{SL}{SL_{max}} - x_{0,L})}}$
B15	Lactation cost	lactation_cost	$M_L = (M_{lm,off} + M_{B,off}) \cdot a_L$
B16	Total energetic demand	total_demands	$M = M_B + M_{lm} + M_P + M_L$
B17	Required intake pre-foraging (assimilation)	total_demands_intake	$IR_i = \frac{M}{AE}$
B18	Fat mass change	target_fat_change	$\dot{m}_{fat} = SL_* - m_{fat}$
B19	Energy needed for storage	needed_energy_balance	$M_{fat} = \begin{cases} \frac{\dot{m}_{fat} \cdot ED_{fat}}{\varepsilon_{fat}}, & \dot{m}_{fat} > 0 \\ \frac{\dot{m}_{fat} \cdot ED_{fat}}{\eta_{fat}}, & \dot{m}_{fat} \leq 0 \end{cases}$
B20	Foraging costs	foraging_costs	$IR_F = (IR_i + M_{fat}) \cdot FE$
B21	Energy intake incl. foraging	energy_intake	$IR_{real} = IR_i + M_{fat} + IR_F$
B22	Energy balance	energy_balance	$EB = IR_{real} - IR_F - IR_i$
B23	Fat mass update	fat_change	$m_{fat} = \begin{cases} \frac{EB \cdot \varepsilon_{fat}}{ED_{fat}} + m_{fat}, & EB > 0 \\ \frac{EB}{ED_{fat} \cdot \eta_{fat}} + m_{fat}, & EB \leq 0 \end{cases}$

B24	Body mass update	new_structural_mass	$m_{lm} = m_{lm} + \frac{M_{lm} DE_m}{ED_m}$
B25	Embryo mass update	emb_mass	$m_{emb} = m_{emb} + \frac{\max(0,\ a_P - M_G)\ DE_m}{ED_m\, n_{off}}$
B26	Offspring mass update	off_mass	$m_{off} = m_{off} + \frac{\max(0,\ a_L - M_{B,off})\ DE_m}{ED_m\, n_{off}}$
B27	Storage level update	new_storage_level	$SL = \frac{m_{fat}}{m_{lm} + m_{fat}}$
B28	Survival probability curve	survival_prob	$\beta_A = \frac{1}{1 + e^{-k_S(\frac{SL}{SL_{max}} - x_{0,S})}}$